We are IntechOpen, the world's leading publisher of Open Access books Built by scientists, for scientists

4,800
Open access books available

122,000
International authors and editors

135M
Downloads

Our authors are among the

154
Countries delivered to

TOP 1%
most cited scientists

12.2%
Contributors from top 500 universities

CLARIVATE ANALYTICS BOOK CITATION INDEX INDEXED

WEB OF SCIENCE™

Selection of our books indexed in the Book Citation Index in Web of Science™ Core Collection (BKCI)

Interested in publishing with us?
Contact book.department@intechopen.com

Numbers displayed above are based on latest data collected.
For more information visit www.intechopen.com

4

Output Feedback Direct Adaptive Control for a Two-Link Flexible Robot Subject to Parameter Changes

Selahattin Ozcelik and Elroy Miranda
Texas A&M University-Kingsville, Texas
USA

1. Introduction

Robots today have an ever growing niche. Many of today's robots are required to perform tasks which demand high level of accuracy in end effector positioning. The links of the robot connecting the joints are large, rigid, and heavy. These manipulators are designed with links, which are sufficiently stiff for structural deflection to be negligible during normal operation. Also, heavy links utilize much of the joint motor's power moving the link and holding them against gravity. Moreover the payloads have to be kept small compared to the mass of the robot itself, since large payloads induce sagging and vibration in the links, eventually bringing about uncertainty in the end effector position. In an attempt to solve these problems lightweight and flexible robots have been developed. These lightweight mechanical structures are expected to improve performance of the robot manipulators with typically low payload to arm weight ratio. The ultimate goal of such robotic designs is to accurate tip position control in spite of the flexibility in a reasonable amount of time. Unlike industrial robots, these robot links will be utilized for specific purposes like in a space shuttle arm. These flexible robots have an increased payload capacity, lesser energy consumption, cheaper construction, faster movements, and longer reach. However, link flexibility causes significant technical problems. The weight reduction leads the manipulator to become more flexible and more difficult to control accurately. The manipulator being a distributed parameter system, it is highly non-linear in nature. Control algorithms will be required to compensate for both the vibrations and static deflections that result from the flexibility. This provides a challenge to design control techniques that:

a) gives precise control of desired parameters of the system in desired time,
b) cope up with sudden changes in the bounded system parameters,
c) gives control on unmodeled dynamics in the form of perturbations, and
d) robust performance.

Conventional control system design is generally a trial and error process which is often not capable of controlling a process, which varies significantly during operation. Thus, the quest for robust and precise control led researchers to derive various control theories. Adaptive control is one of these research fields that is emerging as timely and important class of controller design. Area much argued about adaptive control is its simplicity and ease of

physical implementation on actual real-life systems. In this work, an attempt has been made to show the simplicity, ease and effectiveness of implementation of direct model reference adaptive control (DMRAC) on a multi input multi output (MIMO) flexible two-link system. The plant comprises of a planar two-link flexible arm with rotary joints subject only to bending deformations in the plane of motion. A payload is added at the tip of the outer link, while hub inertias are included at actuated joints. The goal is to design a controller that can control the distal end of the flexible links.

Probably the first work done pertaining to the control of flexible links was presented by (Cannon & Schmitz, 1984). Considering a flexible link, which was only flexible in one dimension (perpendicular to gravity), a Linear Quadratic Gaussian controller was designed for the position control. Direct end point sensing was used and the goal was to execute a robot motion as fast as possible without residual vibrations in the beam. Also, experiments were carried out on end point control of a flexible one link robot. These experiments demonstrated control strategies for position of one end to be sensed and precisely positioned by applying torque at the other end. These experiments were performed to uncover and solve problems related to the control of very flexible manipulators, where sensors are collocated with the actuators.

(Geniele et al., 1995) worked on tip-position control of a single flexible link, which rotates on a horizontal plane. The dynamic model was derived using assumed-modes method based on the Euler-Bernoulli beam theory. The model is then linearized about an operating point. The control strategy for this non-minimum phase linear time varying system consisted of two parts. The first part had an inner stabilizing control loop that incorporates a feedforward term to assign the system's transmission zeros at desired locations in the complex plane, and a feedback term to move the system's poles to the desire positions in the left half plane. In the second part, the other loop had a feedback servo loop that allowed tracking of the desired trajectory. The controller was implemented on an experimental test bed. The performance was then compared with that of a pole placement state feedback controller.

(Park & Asada, 1992) worked on an integrated structure and control design of a two-link non-rigid robot arm for the purpose of high speed positioning. A PD control system was designed for the simple dynamic model minimizing the settling time. Optimal feedback gains were obtained as functions of structural parameters involved in the dynamic model. These parameters were then optimized using an optimization technique for an overall optimal performance.

(Lee et al., 2001) worked on the adaptive robust control design for multi-link flexible robots. Adaptive energy-based robust control was presented for both close loop stability and automatic tuning of the gains for desired performance. A two-link finite element model was simulated, in which each link was divided into four elements of same length. The controller designed was independent of system parameters and hence possessed stability robustness to parameter variations.

Variations in flexible links have also been researched. Control of a two-link flexible arm in contact with a compliant surface was shown in (Scicliano & Villani, 2001). Here, for a given tip position and surface stiffness, the joint and deflection variables are computed using closed loop inverse kinematics algorithm. The computed variables are then used as the set points for a simple joint PD control, thus achieving regulation of the tip position and contact force via a joint-space controller.

(Ider et al., 2002) proposed a new method for the end effector trajectory tracking control of robots with flexible links. In order to cope with the non-minimum phase property of the system, they proposed to place the closed-loop poles at desire locations using full state feedback. A composite control law was designed to track the desired trajectory, while at the same time the internal dynamics were stabilized. A two-link planar robot was simulated to illustrate the performance of the proposed algorithm. Moreover the method is valid for all types of manipulators with any degree of freedom.
(Green, A. & Sasiadek, J., 2004) presented control methods for endpoint tracking of a two-link robot. Initially, a manipulator with rigid links is modeled using inverse dynamics, a linear quadratic regulator and fuzzy logic schemes actuated by a Jacobian transpose control law computed using dominant cantilever and pinned-pinned assumed mode frequencies. The inverse dynamics model is pursued further to study a manipulator with flexible links where nonlinear rigid-link dynamics are coupled with dominant assumed modes for cantilever and pinned-pinned beams. A time delay in the feedback control loop represents elastic wave travel time along the links to generate non-minimum phase response.
An energy-based nonlinear control for a two-link flexible manipulator wasstudied in (Xu et al., 2005). It was claimed that their method can provide more physical insights in nonlinear control as well as provide a direct candidate for the Lyapunov function. Both simulation and experimental results were provided to demonstrate the effectiveness of the controllers
A robust control method of a two-link flexible manipulator with neural networks based quasi-static distortion compensation was proposed in (Li et al., 2005). The dynamics equation of the flexible manipulator was divided into a slow subsystem and a fast subsystem based on the assumed mode method and singular perturbation theory. A decomposition based robust controller is proposed with respect to the slow subsystem, and H_∞ control is applied to the fast subsystem. The proposed control method has been implemented on a two-link flexible manipulator for precise end-tip tracking control.
In this work a direct adaptive controller is designed and the effectiveness of this adaptive control algorithm is shown by considering the parametric variations in the form of additive perturbations. This work emphasizes the robust stability and performance of adaptive control, in the presence of parametric variations. This approach is an output feedback method, which requires neither full state feedback nor adaptive observers. Other important properties of this class of algorithms include:

a) Their applicability to non-minimum phase systems,
b) The fact that the plant (physical system) order may be much higher than the order of the reference model, and
c) The applicability of this approach to MIMO systems.

Its ease of implementation and inherent robustness properties make this adaptive control approach attractive.

2. Mathematical Modeling of the System

In this section mathematical model of the system is derived using Lagrange equations with the assumed-modes method. The links are assumed to obey Euler-Bernoulli beam model with proper boundary conditions. A payload has been added to the tip of the second link, while hub inertias are included at the actuator joints.

2.1 Kinematic Modeling

A planar two-link flexible arm with rotary joints subject to only bending deformations in the plane of motion is considered. The following coordinate frames, as seen in Fig. 1, are established: the inertial frame (X_0, Y_0), the rigid body moving frame associated to link *i* (X_i, Y_i), and the flexible body moving frame associated with link *i* ($\hat{X}_i, \hat{Y}_i$) (Brook, 1984).

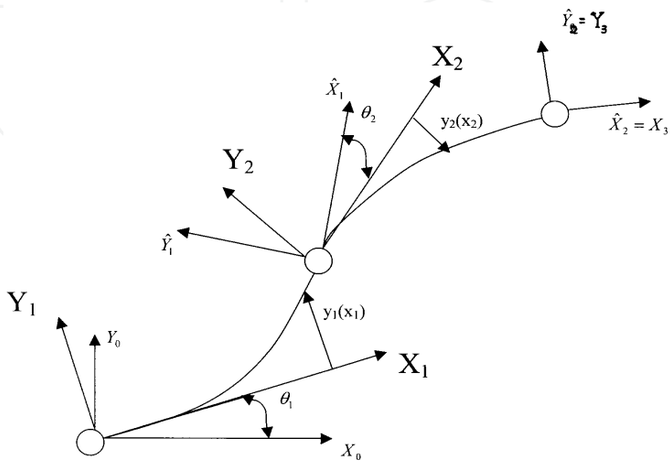

Fig. 1. Planar Flexible Two-Link Arm

The rigid body motion is described by the joint angle, θ_i, while $y_i(x_i)$ denoted the transversal deflection of link *i* at abscissa, $0 \le x_i \le l_i$, l_i being the link length. Let $p_i^i(x_i) = (x_i, y_i(x_i))^T$ be the position of a point along the deflected link *i* with respect to frame (X_i, Y_i) and p_i be the absolute position of the same point on frame (X_0, Y_0). Also, $r_{i+1}^i = p_i^i(l_i)$ indicates the position of the origin of frame (X_{i+1}, Y_{i+1}) with respect to frame (X_i, Y_i), and r_i gives absolute positioning of the origin of frame (X_i, Y_i) with respect to frame (X_0, Y_0). The rotation matrix A_i for rigid body motion and the rotation matrix E_i for the flexible mode are, respectively,

$$A_i = \begin{bmatrix} \cos\theta_i & -\sin\theta_i \\ \sin\theta_i & \cos\theta_i \end{bmatrix} \quad \mathrm{E}_i = \begin{bmatrix} 1 & -y'_{ie} \\ y'_{ie} & 1 \end{bmatrix} \tag{1}$$

where $y'_{ie} = (\delta_{yi} / \delta_{xi})|_{x_i = l_i}$ and for small deflections $\arctan(y'_{ie}) \approx y'_{ie}$. Therefore, the previous absolute position vectors can be expressed as,

$$\mathrm{p}_i = \mathrm{r}_1 + \mathrm{W}_i{}^i \mathrm{p}_i \qquad \mathrm{E}_i = \mathrm{r}_{i+1} = \mathrm{r}_1 + \mathrm{W}_i{}^i \mathrm{r}_{i+1} \tag{2}$$

where, W_i is the global transformation matrix from (X_0, Y_0) to (X_i, Y_i), which obeys the recursive equation $W_i = W_{i-1} E_{i-1} A_i = \hat{W}_{i-1} A_i$ and $\hat{W}_0 = I$

2.2. Lagrangian Modeling

The equations of motion for a planar n-link flexible arm are derived by using the Lagrange equations. The total kinetic energy is given by the sum of the following contributions:

$$T = \sum_{i-1}^{n} T_{hi} + \sum_{i-1}^{n} T_{li} + T_p \tag{3}$$

where the kinetic energy of the rigid body located at the hub *i* of mass m_{hi} and the moment of inertia J_{hi} is

$$T_{hi} = \frac{1}{2} m_{hi} \dot{r}_i + \frac{1}{2} J_{hi} \alpha_i^2 \tag{4}$$

where $\dot{\alpha}_i$ is the (scalar) absolute angular velocity of frame (X_i, Y_i) given by

$$\dot{\alpha}_i = \sum_{j=1}^{1} \dot{\theta}_j + \sum_{k=1}^{i-1} \dot{y}'_{ke} \tag{5}$$

Moreover, the absolute linear velocity of an arm is

$$\dot{p} = \dot{r}_i + \dot{W}_i p_i^i + W_i^i \dot{p}_i \tag{6}$$

and $\dot{r}_{i+1}^i = \dot{p}_i^i(l_i)$. Since the links are assumed inextensible ($\dot{x}_i = 0$), then $\dot{p}_i^i(x_i) = (0, \dot{y}_i(x_i))^T$. The kinetic energy pertaining to link *i* of linear density ρ_i is

$$T_{li} = \frac{1}{2} \int_0^{li} \rho_i(x_i) \dot{p}_i^T(x_i) dx_i \tag{7}$$

and the kinetic energy associated to a payload of mass m_p and moment of inertia J_p located at the end of link *n* is

$$T_p = \frac{1}{2} m_p \dot{r}_{n+1}^T \dot{r}_{n+1} + \frac{1}{2} J_p (\dot{\alpha}_n + \dot{y}'_{ne})^2 \tag{8}$$

Now, in the absence of gravity (horizontal plane motion), the potential energy is given by

$$U = \sum_{i=1}^{n} U_i = \sum_{i=1}^{n} \frac{1}{2} \int_0^{li} (EI)_i(x_i) \left[\frac{d^2 y_i(x_i)}{dx_i^2} \right]^2 dx_i \tag{9}$$

Where U_i is the elastic energy stored in link *i*, and $(EI)_i$ being its flexural rigidity. No

discretization of structural link flexibility has been made so far, so the Lagrangian will be a functional.

2.3. Assumed Mode Shapes

Links are modeled as Euler Bernoulli beams of uniform density ρ_i and constant flexural rigidity $(EI)_i$ with the deformation $y_i(x_i,t)$ satisfying the partial differential equation

$$(EI)_i \frac{\partial^4 y_i(x_i,t)}{\partial x_i^4} + \rho_i \frac{\partial^2 y_i(x_i,t)}{\partial t^2} = 0, i = 1,...,n. \tag{10}$$

Boundary conditions are imposed at the base of and the end of each link to solve this equation. The inertia of a light weight link is small compared to the hub inertia, and then constrained mode shapes can be used. We assume each slewing link to be *clamped* at the base

$$y_i(0,t) = 0, y_i'(0,t) = 0, i = 1,...,n \tag{11}$$

For the remaining boundary conditions it is assumed that the link end is free of dynamic constraints, due to the difficulty in accounting for time-varying or unknown masses and inertias. However, we consider mass boundary conditions representing balance of moment and shearing force, i.e.

$$\begin{aligned}
(EI)_i \left[\frac{\partial^2 y_i(x_{i,t})}{\partial x_i^2}\right]_{x_i=l_i} &= -J_{Li}\frac{d^2}{dt^2}\left[\left(\frac{\partial y_i(x_i,t)}{\partial x_i}\right)_{x_i=l_i}\right] - (MD)_i \frac{d^2}{dt^2}(y_i(x_{i,t})_{x_i=l_i}) \\
(EI)_i \left[\frac{\partial^3 y_i(x_{i,t})}{\partial x_i^3}\right]_{x_i=l_i} &= -M_{Li}\frac{d^2}{dt^2}(y_i(x_{i,t})_{x_i=l_i}) - (MD)_i \frac{d^2}{dt^2}\left[\left(\frac{\partial y_i(x_i,t)}{\partial x_i}\right)_{x_i=l_i}\right] \\
i &= 1,....,n
\end{aligned} \tag{12}$$

where, M_{Li} and J_{Li} are the actual mass and moment of inertia at the end of link *i*. $(MD)_i$ accounts for the contribution of masses of distal links, i.e. non-collocated at the end of link *i*. A finite-dimensional model of link flexibility can be obtained by assumed modes technique. Using this technique the link deflections can be expressed as

$$y_i(x_i,t) = \sum_{j=1}^{m_i} \phi_{ij}(x_i)\delta_{ij}(t) \tag{13}$$

where $\delta_{ij}(t)$ are the time varying variables associated with the assumed spatial mode shapes $\varphi_{ij}(x_i)$ of link *i*. Therefore each term in the general solution of (10) is the product of a time harmonic function of the form

$$\delta_{ij(t)} = \exp(j\omega_{ij}t) \tag{14}$$

and of a space eigenfunction of the form

$$\phi_{ij}(x_i) = C_{1,ij}\sin(\beta_{ij}x_i) + C_{2,ij}\cos(\beta_{ij}x_i) + C_{3,ij}\sinh(\beta_{ij}x_i) + C_{3,ij}\cosh(\beta_{ij}x_i) \tag{15}$$

In (14) ω_{ij} is the *j*th natural angular frequency of the eigenvalue problem for link *i*, and in (15) $\beta_{ij} = \omega_{ij}^2\rho_i/(EI)_i$.

Application of the aforementioned boundary conditions allows the determination of the constant coefficients in (15). The clamped link conditions at the link base yield

$$C_{3,ij} = -C_{1,ij}, C_{4,ij} = -C_{2,ij} \tag{16}$$

while, the mass conditions at the link end lead to homogeneous system of the form

$$\left[F\left(\beta_{ij}\right)\right]\begin{bmatrix} C_{1,ij} \\ C_{2,ij} \end{bmatrix} \tag{17}$$

The so-called frequency equation is obtained by setting to zero the determinant of the (2×2) matrix $F(\beta_{ij})$ that depends on explicitly on the values of M_{Li}, J_{Li}, and $(MD)_i$. The first m_i roots of this equation give the positive values of β_{ij} to be plugged in (15). Using this the coefficients $C_{1,ij}$ and $C_{2,ij}$ are determined up to a scale factor that is chosen via a suitable normalization. Further the resulting eigenfunctions φ_{ij} satisfy a modified orthogonality condition that includes the actual M_{Li}, J_{Li}, and $(MD)_i$. In an open kinematic chain arrangement, M_{Li} is the constant sum of all masses beyond link *i*, but J_{Li} and $(MD)_i$ depend on the position of successive links. This will considerably increase the complexity of model derivation and overload the computational burden of on-line execution. Thus, some practical approximation leading to constant although nonzero boundary conditions at the link end is done. Thus, a convenient position is set to $(MD)_i$ = 0 and compute J_{Li} for a fixed arm configuration. In this case, it can be shown that det(*F*) = 0 results in the following transcendental equation (De Luca & Scicliano, 1989)

$$\begin{aligned}\left(1+\cos\left(\beta_{ij}l_i\right)\cosh\left(\beta_{ij}l_i\right)\right) - \frac{M_{Li}\beta_{ij}}{\rho_i}\left(\sin\left(\beta_{ij}l_i\right)\cosh\left(\beta_{ij}l_i\right) - \cos\left(\beta_{ij}l_i\right)\sinh\left(\beta_{ij}l_i\right)\right) \\ - \frac{J_{Li}\beta_{ij}^3}{\rho_i}\left(\sin\left(\beta_{ij}l_i\right)\cosh\left(\beta_{ij}l_i\right) + \cos\left(\beta_{ij}l_i\right)\sinh\left(\beta_{ij}l_i\right)\right) \\ + \frac{M_{Li}J_{Li}\beta_{ij}^4}{\rho_i^2}\left(1-\cos\left(\beta_{ij}l_i\right)\cosh\left(\beta_{ij}l_i\right)\right) = 0\end{aligned} \tag{18}$$

2.4. Closed-Form Equations of Motion

On the basis of the discretization introduced in the previous section, the Lagrangian L becomes a function of set of N generalized coordinates $q_i(t)$ the dynamic model is obtained satisfying the Lagrange-Euler equations

$$\frac{d}{dt}\left(\frac{\partial L}{\partial \dot{q}_i}\right)-\frac{\partial L}{\partial q_i}=f_{i,} \qquad i=1\cdots N \tag{19}$$

where, f_i are the generalized forces performing work on $q_i(t)$. Under the assumption of constant mode shapes, it can be shown that spatial dependence present in the kinetic energy term (7) can be resolved by the introduction of a number of constant parameters, characterizing the mechanical properties of the (uniform density) links (De Luca, et. al. 1988, Cetinkunt, et. al., 1986)

$$m_i=\int_0^{li}\rho_i dx_i=\rho_i l_i \tag{20}$$

$$d_i=\frac{1}{m_i}\int_0^{li}\rho_i x_i x_i=\frac{1}{2}l_i \tag{21}$$

$$J_{0i}=\int_0^{li}\rho_i x_i^2 dx_i=\frac{1}{3}m_i l_i^2 \tag{22}$$

$$v_{ij}=\int_0^{li}\rho_i\varphi_{ij}\left(x_i\right)dx_i \tag{23}$$

$$w_{ij}=\int_0^{li}\rho_i\varphi_{ij}\left(x_i\right)x_i dx_i \tag{24}$$

$$z_{ijk}=\int_0^{li}\rho_i\varphi_{ij}\left(x_i\right)\varphi_{ik}\left(x_i\right)dx_i \tag{25}$$

$$k_{ijk}=\int_0^{li}(EI)_i\varphi_{ij}\left(x_i\right)\varphi_{ik}\left(x_i\right)dx_i \tag{26}$$

where, m_i is the mass of the link i, d is the distance of center of mass of link i from joint i axis, J_{0i} is the inertia of link i about joint i axis, v_{ij} and ω_{ij} are the deformation moments of order zero and one of mode j of the link i. Also, k_{ijk} is the cross elasticity coefficient of modes j and k of link i. The actual numerical values of the previous parameters are calculated off-line. As a result of this procedure, the equations of motion for a planar n-link arm can be written in a familiar closed form

$$B(q)\ddot{q}+h(q,\dot{q})+Kq=Qu \tag{27}$$

where $q = \left(\theta_1\ \theta_n\ \delta_{11}\ \delta_{1,m_1}\ \delta_{n,1}\ \delta_{n,m_n}\right)^T$ is the *N*-vector of generalized coordinates ($N = n + \sum_i m_i$), and *u* is the *n*-vector of joint actuator torques. *B* is the positive definite symmetric inertia matrix, *h* is the vector of Corriolis and centrifugal forces, *K* is the stiffness matrix and *Q* is the input weighting matrix that is of the form $\left[I_{nxn}\ O_{nx(N-n)}\right]^T$ due to the clamped link assumptions. Joint viscous friction and link structural damping can be added as $D\dot{q}$, where *D* is a diagonal matrix. It is noted that orthonormalization of mode shapes implies convenient simplification in the diagonal blocks of the inertia matrix relative to the deflections of each link, due to the particular values attained by z_{ijk} in (25). Also the stiffness matrix becomes diagonal $\left(K_1 = \cdots = K_n = 0; K_{n+1}, \ldots, K_N > 0\right)$ being $k_{ijk} = 0$ for $j \neq k$ in (27). The components of *h* can be evaluated through the Christoffel symbols given by

$$h_i = \sum_{j=1}^{N}\sum_{k=1}^{N}\left(\frac{\partial B_{ij}}{\partial q_k} - \frac{1}{2}\frac{\partial B_{jk}}{\partial q_j}\right)\dot{q}_j\dot{q}_k \tag{28}$$

2.5. Explicit Dynamic Model of Two-Link Flexible Arm

Two assumed mode shapes are considered for each link ($m_1 = m_2 = 2$). Thus, the vector of Lagrangian coordinates reduces to $q = \left(\theta_1\ \theta_2\ \delta_{11}\ \delta_{12}\ \delta_{21}\ \delta_{22}\right)^T$, i.e. *N* = 6. It can be shown (Brook, 1984, De Luca et. al. 1988) that the contributions of kinetic energy due to deflection variables are

$$\left\{factor\ of\ \dot{\delta}_{i1}^2\right\} = z_{i11} \tag{29}$$

$$\left\{factor\ of\ 2\dot{\delta}_{i1}\dot{\delta}_{i2}\right\} = \begin{bmatrix}\varphi_{i1,e} & \varphi'_{i1,e}\end{bmatrix}\begin{bmatrix}M_{Li} & \frac{1}{2}(MD)_i \\ \frac{1}{2}(MD)_i & J_{Li}\end{bmatrix}\begin{bmatrix}\varphi_{i2,e} \\ \varphi'_{i2,e}\end{bmatrix} + z_{i12} \tag{30}$$

$$\left\{factor\ of\ \dot{\delta}_{i2}^2\right\} = z_{i22} \tag{31}$$

where, $\varphi_{ij,e} = \varphi_{ij}(x_i)|_{x_i = l_i}$ and $\varphi'_{ij,e} = \varphi'_{ij}(x_i)|_{x_i = l_i}$, $i, j = 1, 2$. The above equations are obtained expanding terms (7) and (8) by using (5) and (6). Accounting for separability (13) then leads to expressions for the factors of the quadratic deflection rate terms, in which parameters defined in (25) and the mass coefficients on the right hand side of (12) can be identified. It is found for link-1:

$$M_{L1} = m_2 + m_{h2} + m_p \tag{32}$$

$$J_{L1} = J_{02} + J_{h2} + J_p + m_P l_2^2 \tag{33}$$

$$(MD)_1 = \left(m_2 d_2 + m_p l_2\right)\cos\theta_2 - \left[\left(v_{21} + m_p\varphi_{21,e}\right)\delta_{21} + \left(v_{22} + m_p\varphi_{22,e}\right)\delta_{22}\right]\sin\theta_2 \tag{34}$$

Note that in the case of only two links, J_{L1} is a constant. On the other hand for link-2:

$$M_{L2} = m_p, \quad J_{L2} = J_p, \quad (MD)_2 = 0 \tag{35}$$

A convenient normalization of mode shapes is accomplished by setting:

$$z_{iii} = m_i, \quad i, j = 1, 2 \tag{36}$$

This also implies that the nonzero coefficients in the stiffness matrix *K* take on values $w_{ij}^2 m_i$. It is stressed that, if the exact values for the boundary conditions in (12) were used the natural orthogonality of the computed mode shapes would imply that $\{ factor\ of\ 2\dot{\delta}_{11}\dot{\delta}_{12} \}$ is zero for both links. For link-2 the use of (35) automatically ensures the "correct" orthogonality of mode shapes. On the other hand, however for link-1, the off-diagonal term $(MD)_1$ varies with arm configuration. This implies that the mode shapes– which are *spatial* quantities–would become implicit functions of time, thus conflicting with the original separability assumption. It is seen that for different positions of second link, $(MD)_1$ results in variations of (34), so the actual mode shapes of the first link become themselves functions of time-varying variables describing the deflection of the second link. A common approximation in computing the elements of the inertia matrix for flexible structures is to evaluate kinetic energy in correspondence to the undeformed configuration. In our case, it is equivalent to neglecting the second term $(MD)_1$ in (34), which is an order of magnitude smaller than the first term. Accordingly, $(MD)_1$ is constant for a fixed arm configuration. Taking $\theta_2 = \pm\pi/2$ leads to $(MD)_1 = 0$ and thus the eigen-frequencies can be computed through (19). This is equivalent to having zeroed only that portion of the $\{ factor\ of\ 2\dot{\delta}_{11}\dot{\delta}_{12} \}$ generated by constant diagonal terms, i.e.

$$\begin{bmatrix} \varphi_{11,e} & \varphi'_{11,e} \end{bmatrix} \begin{bmatrix} M_{Li} & 0 \\ 0 & J_{Li} \end{bmatrix} \begin{bmatrix} \varphi_{12,e} \\ \varphi'_{12,e} \end{bmatrix} + z_{112} = 0 \tag{37}$$

This will produce nonzero off-diagonal terms in the relative block of the inertia matrix. The resulting model is cast in a computational advantageous form, where a set of constant coefficients appear that depend on the mechanical properties of the arm. The inertia matrix as well as other derivations can be found in (Miranda, 2004). Once having obtained the expressions of the inertia matrix, the components of *h* can be evaluated using (28). Viscous friction and passive structural damping are included in matrix *D* for improvement in arm movement, and finally, the stiffness matrix *K* is of the form,

$$K = diag \left\{ 0,\ 0,\ w_{11}^2 m_1,\ w_{12}^2 m_1,\ w_{21}^2 m_2,\ w_{22}^2 m_2 \right\} \tag{38}$$

Then the equations of motion is given in its standard form as

$$B(q)\ddot{q} + h(q, \dot{q}) + D\dot{q} + Kq = Qu \tag{39}$$

After tremendous of algebra and neglecting friction, (39) can be written as,

$$\begin{aligned}
B_{11}\,\ddot{\theta}_1 + B_{12}\,\ddot{\theta}_2 + B_{13}\,\ddot{\delta}_{11} + B_{14}\,\ddot{\delta}_{12} + B_{15}\,\ddot{\delta}_{21} + B_{16}\,\ddot{\delta}_{22} + h_1 &= u_{p1}\\
B_{21}\,\ddot{\theta}_1 + B_{22}\,\ddot{\theta}_2 + B_{23}\,\ddot{\delta}_{11} + B_{24}\,\ddot{\delta}_{12} + B_{25}\,\ddot{\delta}_{21} + B_{26}\,\ddot{\delta}_{22} + h_2 &= u_{p2}\\
B_{31}\,\ddot{\theta}_1 + B_{32}\,\ddot{\theta}_2 + B_{33}\,\ddot{\delta}_{11} + B_{34}\,\ddot{\delta}_{12} + B_{35}\,\ddot{\delta}_{21} + B_{36}\,\ddot{\delta}_{22} + h_3 + K_3\,\delta_{11} &= 0\\
B_{41}\,\ddot{\theta}_1 + B_{42}\,\ddot{\theta}_2 + B_{43}\,\ddot{\delta}_{11} + B_{44}\,\ddot{\delta}_{12} + B_{45}\,\ddot{\delta}_{21} + B_{46}\,\ddot{\delta}_{22} + h_4 + K_4\,\delta_{12} &= 0\\
B_{15}\,\ddot{\theta}_1 + B_{52}\,\ddot{\theta}_2 + B_{53}\,\ddot{\delta}_{11} + B_{54}\,\ddot{\delta}_{12} + B_{55}\,\ddot{\delta}_{21} + B_{56}\,\ddot{\delta}_{22} + h_2 + K_5\,\delta_{21} &= 0\\
B_{61}\,\ddot{\theta}_1 + B_{62}\,\ddot{\theta}_2 + B_{63}\,\ddot{\delta}_{11} + B_{64}\,\ddot{\delta}_{12} + B_{65}\,\ddot{\delta}_{21} + B_{66}\,\ddot{\delta}_{22} + h_2 + K_6\,\delta_{22} &= 0
\end{aligned} \tag{40}$$

where, u_{p1} and u_{p2} are input torques to joints 1 and 2, respectively. Plant outputs are considered to be link tip displacements y_1 and y_2. As seen from above equations, the system is highly nonlinear and of 12th order. For the flexible robot, the following physical parameters were considered

$$\begin{gathered}
\rho_1 = \rho_2 = 0.2\ kg/m\\
l_1 = l_2 = 0.5\ m,\ d_2 = 0.25\ m\\
m_1 = m_2 = m_p = 0.1\ kg,\ m_{h2} = 1\ kg\\
J_{01} = J_{02} = 0.0083\ kgm^2\\
J_{h1} = J_{h2} = 0.1\ kgm^2,\ J_p = 0.0005\ kgm^2\\
(EI)_1 = (EI)_2 = 1\ Nm^2
\end{gathered} \tag{41}$$

The natural frequencies $f_{ij} = w_{ij}/2\pi$ and the remaining parameters in the model coefficients are computed as (Miranda, 2004):

$$\begin{gathered}
f_{11} = 0.48\ Hz,\ f_{12} = 1.80\ Hz,\\
f_{21} = 2.18\ Hz,\ f_{22} = 15.91\ Hz,\\
\varphi_{11,e} = 0.186,\ \varphi_{12,e} = 0.215,\ \varphi'_{11,e} = 0.657,\ \varphi'_{12,e} = -0.560,\\
\varphi_{21,e} = 0.883,\ \varphi_{22,e} = -0.069,\ \varphi'_{21,e} = 2.641,\ \varphi'_{22,e} = -10.853,\\
v_{11} = 0.007,\ v_{12} = 0.013,\ v_{21} = 0.033,\ v_{22} = 0.054,\\
w_{11} = 0.002,\ w_{12} = 0.004,\ w_{21} = 0.012,\ w_{22} = 0.016
\end{gathered} \tag{42}$$

In order to design the proposed adaptive controller, the plant needs to be linearized and the transfer function matrix be obtained. After linearization, neglecting higher order terms, and tremendous amount of algebra, it can be shown (Miranda, 2004) that the plant $G_{po}(s) = y_p(s)/u_p(s)$ with nominal parameters can be obtained as,

$$G_{p0}(s) = \begin{bmatrix} y_{p1}(s) \\ y_{p2}(s) \end{bmatrix} \begin{bmatrix} \dfrac{0.01641s^{10} + 7.061*10^{-5}\ s^8}{s^{12} + 3.68*10^{-3}\ s^{10}} & \dfrac{-2.259s^{10} - 1.362*10^{-3}\ s^8}{s^{12} + 3.68*10^{-3}\ s^{10}} \\ \dfrac{-7.357s^{10} - 9.636*10^{-3}\ s^8}{s^{12} + 3.68*10^{-3}\ s^{10}} & \dfrac{1317\ s^{10} + 0.674s^8}{s^{12} + 3.68*10^{-3}\ s^{10}} \end{bmatrix} \begin{bmatrix} u_{p1}(s) \\ u_{p2}(s) \end{bmatrix} \tag{43}$$

where, $G_{po}(s)$ is the nominal plant transfer function matrix. Now, performing minimal realization, $G_{po}(s)$ can be reduced to

$$G_{po}(s)=\begin{bmatrix} \dfrac{0.01641s^2+7.061*10^{-5}}{s^4+3.68*10^{-3}\,s^2} & \dfrac{-2.259s^2-1.362*10^{-3}}{s^4+3.68*10^{-3}\,s^2} \\ \dfrac{-7.357s^2-9.636*10^{-3}}{s^4+3.68*10^{-3}\,s^2} & \dfrac{1317s^2+0.674}{s^4+3.68*10^{-3}\,s^2} \end{bmatrix} \tag{44}$$

From (44), it is straight forward to obtain the actual plant in general form as

$$G_p(s)=\frac{y_p(s)}{u_p(s)}=\begin{bmatrix} \dfrac{C_1^{11}\,s^2+C_0^{11}}{s^4+B_2^{11}\,s^2} & \dfrac{C_1^{12}\,s^2+C_0^{12}}{s^4+B_2^{12}\,s^2} \\ \dfrac{C_1^{21}\,s^2+C_0^{21}}{s^4+B_2^{21}\,s^2} & \dfrac{C_1^{22}\,s^2+C_0^{22}}{s^4+B_2^{22}\,s^2} \end{bmatrix} \tag{45}$$

where, above coefficients of $G_p(s)$ are functions of plant parameters and can vary with the range as defined below:

$$\begin{cases} \underline{C}_{p-j}^{ij} \le C_{p-j}^{ij} \le \overline{C}_{p-j}^{ij} & i=1,2, \quad j=1,2 \\ \underline{B}_{r-j}^{ij} \le B_{r-j}^{ij} \le \overline{B}_{r-j}^{ij} & i=1,2, \quad j=1,2 \end{cases} \tag{46}$$

The values of the nominal plant parameters are defined in the following table. The range considered for each parameter is ±30%.

Parameter	Nominal	Range
C_1^{11}	0.01641	0.011487 *to* 0.02133
C_0^{11}	$7.061*10^{-5}$	$4.9427*10^{-5}$ *to* $9.1793*10^{-5}$
$B_2^{11}=B_2^{12}=B_2^{21}=B_2^{22}$	$3.68*10^{-3}$	$2.576*10^{-3}$ *to* $4.784*10^{-3}$
C_1^{12}	2.259	1.5813 *to* 2.9367
C_0^{12}	$1.362*10^{-3}$	$9.583*10^{-4}$ *to* $1.7797*10^{-3}$
C_1^{21}	7.357	5.1499 *to* 9.5641
C_0^{21}	$9.636*10^{-3}$	$6.7452*10^{-1}$ *to* $12.5268*10^{-3}$
C_1^{22}	1317	921.9 *to* 1712.1
C_0^{22}	0.674	0.4718 *to* 0.8762

Table 1. Plant parameters, nominal values, and variation range.

For comparison reasons, uncompensated response of the nominal plant is given below

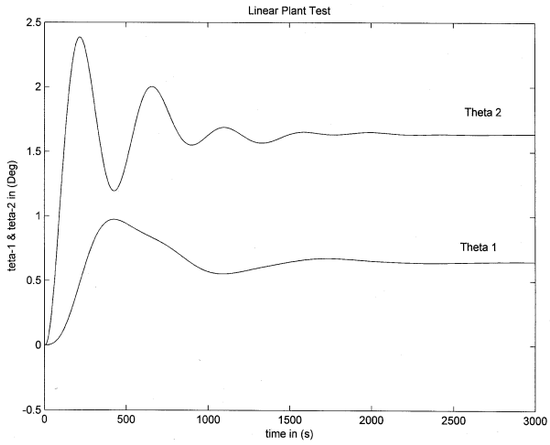

Fig. 2. Uncompensated response of the nominal plant

3. Controller Design

Consider now that the plant given by (45) is represented by the following state-space equations:

$$\begin{aligned} \dot{x}_p(t) &= A_p x_p(t) + B_p u_p(t) \\ y_p(t) &= C_p x_p(t) \end{aligned} \tag{47}$$

where $x_p(t)$ is the (n ×1) state vector, $u_p(t)$ is the (m×1) control vector, $y_p(t)$ is the (q × 1) plant output vector, and A_p, B_p and C_p are matrices with appropriate dimensions. The range of the plant parameters given by (46) is now given by

$$\begin{aligned} \underline{a}_{ij} \le a_p(i,j) \le \bar{a}_{ij}, i, j = 1, \ldots, n \\ \underline{b}_{ij} \le b_p(i,j) \le \bar{b}_{ij}, i, j = 1, \ldots, n \end{aligned} \tag{48}$$

where $a_p(i, j)$ is the $(i, j)^{th}$ element of A_p and $b_p(i, j)$ is the $(i, j)^{th}$ element of B_p. Consider also the following reference model, for which plant output is expected to follow the model output without explicit knowledge of A_p and B_p.

$$\begin{aligned} \dot{x}_m(t) &= A_m x_m(t) + B_m u_m(t) \\ y_m(t) &= C_m x_m(t) \end{aligned} \tag{49}$$

In light of this objective, consider now the following output feedback adaptive control law,

$$u_p(t) = K_e(t) e_y(t) + K_x(t) x_m(t) + K_u(t) u_m(t) \tag{50}$$

where $e_y(t) = y_m(t) - y_p(t)$ and $K_e(t)$, $K_x(t)$, and $K_u(t)$ are adaptive gains defined below. The control law consists of a feedback term from output error and a feedforward terms from model states and inputs. The adaptive gains $K_e(t)$, $K_x(t)$, and $K_u(t)$ are combination of proportional and integral gains as given below,

$$K_j(t) = K_{pj}(t) + K_{ij}(t) \quad j = e, x, u \tag{51}$$

and they are updated according to the following adaptation law (Kaufman, et. al. 1998, Ozcelik & Kaufman, 1999)

$$K_{pj}(t) = e_y(t)[e_y(t) + x_m(t) + u_m(t)]T_p \quad j = e, x, u, T_p \geq 0 \tag{52}$$

$$K_{ij}(t) = e_y(t)[e_y(t) + x_m(t) + u_m(t)]T_i \quad j = e, x, u, \ T_i > 0 \tag{53}$$

where T_i and T_p are constant proportional and integral weighting matrices, respectively. It is seen from (53) that the term $K_{ij}(t)$ is a perfect integrator and may steadily increase whenever *perfect* following ($e_y(t) = 0$) is not possible. The gain may reach unnecessarily large values, or may even diverge. Thus, a σ-term is introduced in order to avoid the divergence of integral gains (Ionnou & Kokotovic, 1983). With the σ -term, $K_i(t)$ is now from a first-order filtering of $e_y(t)r^T(t)T_i$ and therefore cannot diverge, unless $e_y(t)$ diverges. However, in this context, the σ -term does more for the concept of '*adaptive control*'. The gains increase only if high gains are needed and decrease if they are not needed any more. They are also allowed to change at any rate without affecting stability, such that the designer can adjust this rate to fit the specific needs of the particular plant. Thus, using σ -term we rewrite the equation (53) as follows,

$$K_{ij}(t) = e_y(t)[e_y(t) + x_m(t) + u_m(t)]T_i - \sigma K_{ij}(t) \quad j = e, x, u \tag{54}$$

For this adaptive control to work and for asymptotic tracking to be achieved, the plant is required to be almost strictly positive real (ASPR) (Bar-Kana, 1994); that is, there exists a gain matrix K_e, not needed for implementation, such that the closed-loop transfer function

$$G_c(s) = [I + G_p(s)K_e]^{-1} G_p(s) \tag{55}$$

is strictly positive real (SPR). And that it can be shown that (Kaufman, et. al., 1998) a MIMO system represented by a transfer function $G_p(s)$ is ASPR if it:

a) is minimum phase (zeros of the transfer function are on the left-half plane),
b) has relative degree of m or zero (i.e., the difference in the degree of denominator and numerator, (n-m=m) or (n-m=0)), and
c) has minimal realization with high frequency gain $C_pB_p > 0$ (positive definite).

Obviously, the plant given by (45) does not satisfy the so-called ASPR conditions and that can not be applied. However, it has been shown in (Kaufman, et. al., 1998) and (Ozcelik,

2004) that there exist a feedforward compensator $H(s)$ such that the augmented plant $G_a(s) = G_p(s) + H(s)$ is ASPR and the proposed adaptive algorithm can be implemented confidently.

3.1. Design of a Feedforward Compensator (FFC) for the Flexible Robot

From the above restrictions it is obvious that the plant given by (45) is not ASPR and that an FFC has to be designed. Now consider the actual plant $G_p(s)$ again,

$$G_p(s) = \begin{bmatrix} \dfrac{C_1^{11}s^2 + C_0^{11}}{s^4 + B_2^{11}s^2} & \dfrac{C_1^{12}s^2 + C_0^{12}}{s^4 + B_2^{12}s^2} \\ \dfrac{C_1^{21}s^2 + C_0^{21}}{s^4 + B_2^{21}s^2} & \dfrac{C_1^{22}s^2 + C_0^{22}}{s^4 + B_2^{22}s^2} \end{bmatrix} \tag{56}$$

Assuming that the nominal plant parameters are known, the parametric uncertainty of the plant can be transformed into a frequency dependent additive perturbation of the plant by representing of the actual plant $G_p(s)$ as $G_p(s) = G_{p0}(s) + \Delta_a(s)$, with $G_{p0}(s)$ being a nominal plant and $\Delta_a(s)$ being a frequency dependent additive perturbation. Then, one can write

$$\Delta_a(s) = G_p(s) - G_{p0}(s) \tag{57}$$

From (57), the additive uncertainty transfer function can be obtained as

$$\Delta_a(s) = \begin{bmatrix} \lambda_{11}(s) & \lambda_{12}(s) \\ \lambda_{21}(s) & \lambda_{22}(s) \end{bmatrix} \tag{58}$$

where,

$$\begin{aligned}
\lambda_{11}(s) &= \frac{(C_1^{11} - 0.01641)s^6 + \left(3.68*10^{-3}C_1^{11} + C_0^{11} - 7*10^{-5} - 0.01641B_2^{11}\right)s^4 + \left(3.68*10^{-3}C_0^{11} - 7*10^{-5}B_2^{11}\right)s^2}{s^8 + \left(3.68*10^{-3} + B_2^{11}\right)s^6 + B_2^{11}3.68*10^{-3}s^4} \\
\lambda_{12}(s) &= \frac{(2.25 + C_1^{12})s^6 + \left(3.68*10^{-3}C_1^{12} + C_0^{12} + 1.36*10^{-3} + 2.25B_2^{12}\right)s^4 + \left(3.68*10^{-3}C_0^{12} + 1.36*10^{-3}B_2^{12}\right)s^2}{s^8 + \left(3.68*10^{-3} + B_2^{12}\right)s^6 + b_1 3.68*10^{-3}s^4} \\
\lambda_{21}(s) &= \frac{(7.32 + C_1^{21})s^6 + \left(3.68*10^{-3}C_1^{21} + C_0^{21} + 9.63*10^{-3} + 7.35B_2^{21}\right)s^4 + \left(3.68*10^{-3}C_0^{21} + 9.63*10^{-3}B_2^{21}\right)s^2}{s^8 + \left(3.68*10^{-3} + B_2^{21}\right)s^6 + b_1 3.68*10^{-3}s^4} \\
\lambda_{22}(s) &= \frac{(C_1^{22} - 1317)s^6 + \left(3.68*10^{-3}C_1^{22} + C_0^{22} - 0.674 - 1317B_2^{21}\right)s^4 + \left(3.68*10^{-3}C_0^{22} - 0.674B_2^{21}\right)s^2}{s^8 + \left(3.68*10^{-3} + B_2^{21}\right)s^6 + B_2^{21}3.68*10^{-3}s^4}
\end{aligned} \tag{59}$$

It is seen that the uncertainty is a function of plant parameters, which vary in a given range. Thus, in the design of a feedforward compensator, the worst case uncertainty should be taken into account. To this effect, the following optimization procedure is considered for determining the worst case uncertainty at each frequency (suitable number of discrete values). Define a vector whose elements are plant parameters, i.e.

$$v = \begin{bmatrix} C_p^{ij} & C_{p-1}^{ij} & \cdots & C_0^{ij} & B_r^{ij} & B_{r-1}^{ij} & \cdots & B_0^{ij} \end{bmatrix} \tag{60}$$

Then

$$\underbrace{\text{maximize}}_{v} \left|\lambda_{ij}(jw)\right| \quad at\ each\ w$$
$$subject\ to: \begin{cases} \underline{C}_{p-j}^{ij} \le C_{p-j}^{ij} \le \overline{C}_{p-j}^{ij} \\ \underline{B}_{r-j}^{ij} \le B_{r-j}^{ij} \le \overline{B}_{r-j}^{ij} \end{cases} \tag{61}$$

where λ_{ij} is the ij^{th} element of $\Delta(jw)$. In other words, this optimization is performed for each element of $\Delta(jw)$. After having obtained the worst case (maximum) perturbation, we will assume that the perturbation is not exactly known but its upper bound is known. In other words, there exists a known rational function as an upper bound of the worst case uncertainty. Now the upper bound is characterized by an element by element interpretation, where the upper bound means that each entry of $\lambda(jw)$ is replaced by its corresponding bound. In other words, given the worst case uncertainty for each $\lambda(jw)$, it is assumed that there exists a known rational function $w_{ij}(s) \in RH_\infty$ such that

$$\left|w_{ij}(jw)\right| \ge \max\left|\lambda_{ij}(jw)\right| \forall w \tag{62}$$

Knowing that the plant parameters can vary within their lower and upper bounds, this parametric uncertainty is formulated as an additive perturbation in the transfer function matrix. It is important to note that the controller be designed with respect to worst case uncertainty for each λ_{ij}. This can be achieved by performing an optimization procedure given by (61) for 200 frequencies. Here an element by element uncertainty bound model is used for the characterization of upper bound of the uncertainty matrix. Then w_{ij} , which satisfies (62) for each λ_{ij} is given in matrix form as,

$$W(s) = \begin{bmatrix} \dfrac{7*10^2}{800s^2 + 22s + 0.05} & \dfrac{9*10^4}{80s^2 + 4s + 0.05} \\ \dfrac{425*10^3}{150s^2 5.75s + 0.05} & \dfrac{2*10^9}{25s^2 + 3.75s + 0.125} \end{bmatrix} \tag{63}$$

The magnitude responses for each $max(|\lambda_{ij}|)$ and the corresponding $(|w_{ij}|)$ are given in Figures 3-6. Having obtained the nominal plant and formulated unmodeled dynamics, let's have the following assumptions on the plant,

Assumption 1:

a) The nominal plant parameters are known.
b) The off-diagonal elements of $G_{po}(s)$ and $\Delta_a(s)$ are strictly proper.
c) $\Delta_a(s) \in RH_\infty^{mxm}$ and satisfies (62)

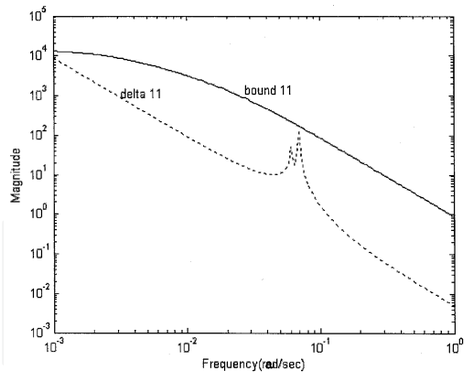

Fig. 3. $|\lambda_{11}(jw)|$ and $|w_{11}(jw)|$

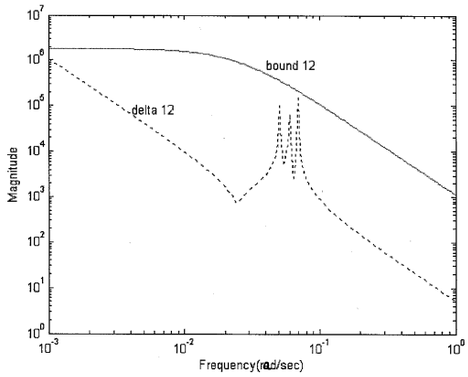

Fig. 4. $|\lambda_{12}(jw)|$ and $|w_{12}(jw)|$

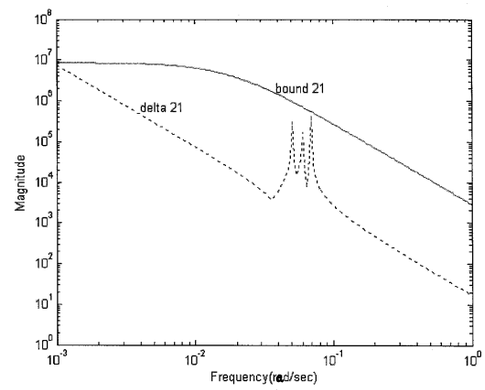

Fig. 5. $|\lambda_{21}(jw)|$ and $|w_{21}(jw)|$

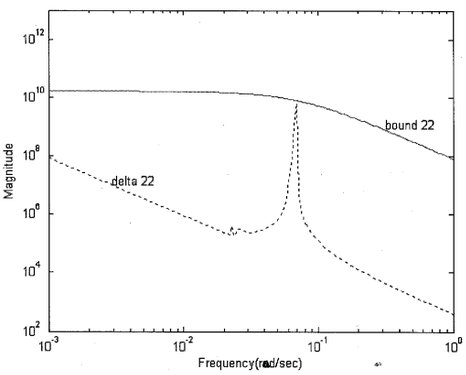

Fig. 6. $|\lambda_{22}(jw)|$ and $|w_{22}(jw)|$

Now, consider the augmented nominal plant with the parallel feedforward compensator

$$G_{ao}(s) = G_{po}(s) + H(s) \tag{64}$$

and the following lemma

Lemma 1:
Let the feedforward compensator H(s) be of the form,

$$H(s) = \begin{bmatrix} h_{11} & 0 & \dots & 0 \\ 0 & h_{22} & \cdots & 0 \\ \vdots & \vdots & \ddots & \vdots \\ 0 & 0 & \dots & h_{mm} \end{bmatrix} \tag{65}$$

with each element $h_{ii}(s)$ of a feedforward compensator being relative degree zero, then the augmented nominal plant $G_{ao}(s) = G_{po}(s)+H(s)$ will have positive definite high frequency gain and relative McMillan degree zero (Ozcelik & Kaufman, 1999).

In other words, the new plant $G_{ao}(s)$ including $H(s)$ becomes ASPR. Now that the ASPR conditions are satisfied for the nominal plant case, we next need to guarantee that the ASPR conditions are also satisfied in the presence of plant perturbations. To this effect, consider the following theorem

Theorem 1: *If $H(s)$ is designed according to the following conditions, then the augmented plant $G_a(s) = G_p(s)+H(s)$ with the plant perturbations will be ASPR.*

a) $H(s)$ is stable with each h_{ij} (s) being relative degree zero

b) H^{-1} (s) stabilizes the nominal closed loop system

c) $\tilde{\Delta}(s) \in RH_\infty$ *and* $\left\|\tilde{\Delta}(s)\right\|_\infty < 1$

where $\tilde{\Delta}(s)$ *is the uncertainty of the augmented plant and given in the following* (Ozcelik & Kaufman, 1999)

$$\tilde{\Delta}(s) = \left(G_{p0}(s) + H(s)\right)^{-1} W(s) \tag{66}$$

In light of the Theorem 1, we can readily determine the FFC as follows:

a) The order of each element $h_{ii}(s)$ of a feedforward compensator is chosen to be equal to the order of the corresponding diagonal element of the nominal plant $G_{p0}(s)$.

$$H(s) = \begin{bmatrix} \dfrac{h_1 s^4 + h_2 s^3 + h_3 s^2 + h_4 s + h_5}{s^4 + 4s^3 + 6s^2 + 4s + 1} & 0 \\ 0 & \dfrac{h_6 s^4 + h_7 s^3 + h_8 s^2 + h_9 s + h_{10}}{s^4 + 4s^3 + 6s^2 + 4s + 1} \end{bmatrix} \tag{67}$$

Denominator of the compensator $H(s)$ appears in the numerator of the closed-loop transfer function and therefore, can be pre-determined such that its time constant is fast enough that its dynamics is negligible.

b) Compensator parameters are determined from the following optimization procedure:

$$\begin{aligned} &\underbrace{\text{minimize}}_{X} \left\|\tilde{\Delta}(jw)\right\|_\infty \\ &subject\ to: \ \text{Re}al\left[roots(Z(s))\right] < 0 \end{aligned} \tag{68}$$

where $Z(s)$ is the characteristic polynomial of the nominal closed-loop system matrix and X is a vector composed of the parameters of each $H_{ij}(s)$.

$$\begin{aligned} &numerator\ of\ h_{11} = 3.7444e^{-4}s^4 + 4.6805e^{-4}s^3 + 9.5966e^{-3}s^2 + 1.1650e^{-3}s + 4.0310e^{-4} \\ &numerator\ of\ h_{22} = 9.2748e^{-5}s^4 + 5.7746e^{-4}s^3 + 2.3495e^{-4}s^2 + 2.9786e^{-5}s + 5.6472e^{-4} \end{aligned} \tag{69}$$

With this FFC, all the conditions of Theorem 1 are satisfied. Thus, the augmented plant satisfies the almost strictly positive real conditions over a wide range of plant parameter variations. It is expected that the DMRAC augmented with this feedforward compensator will be robust for the maximum deviations from the nominal plant. The block diagram of the overall control system is depicted in Figure 7.

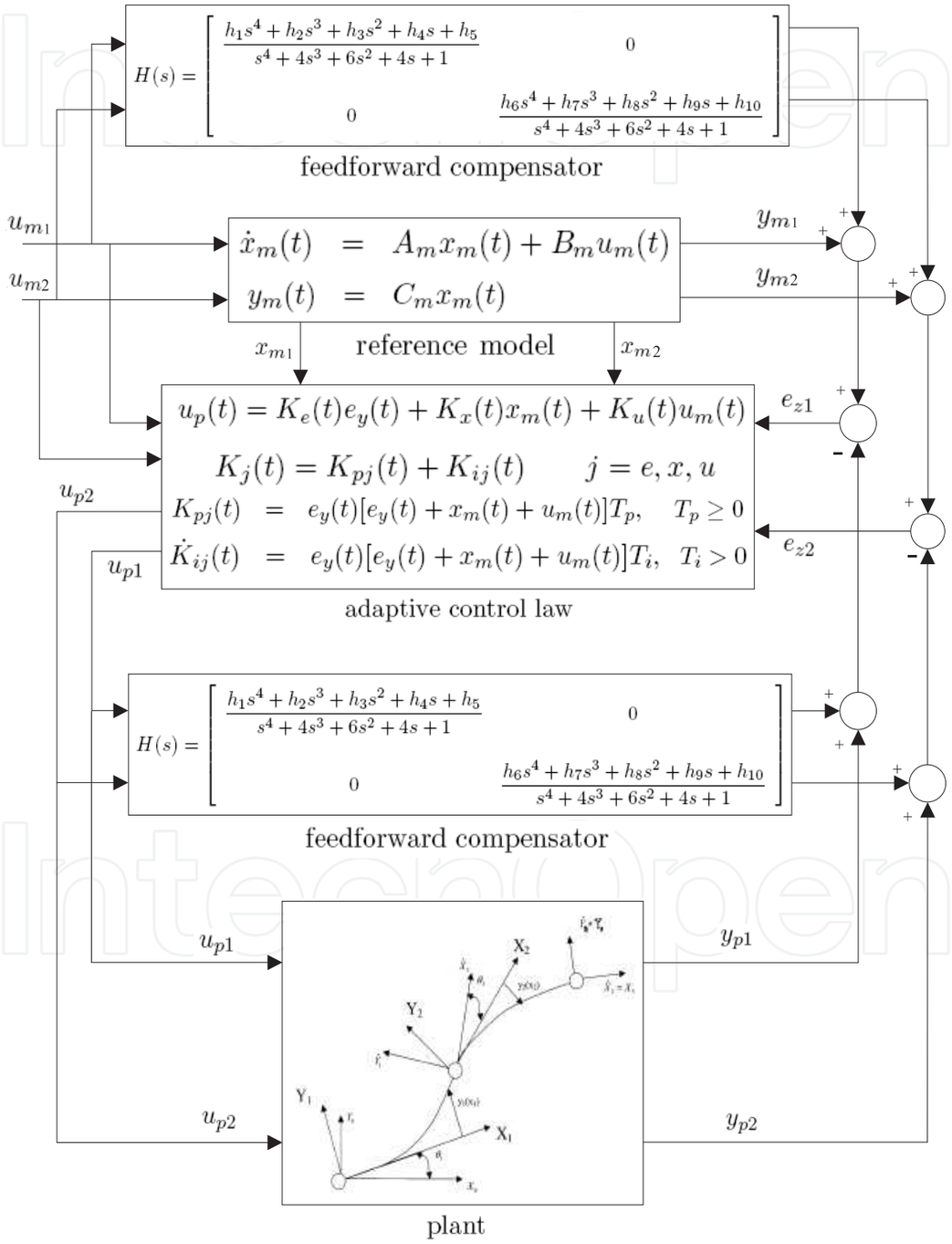

Fig. 7. DMRAC with Two-Link Arm

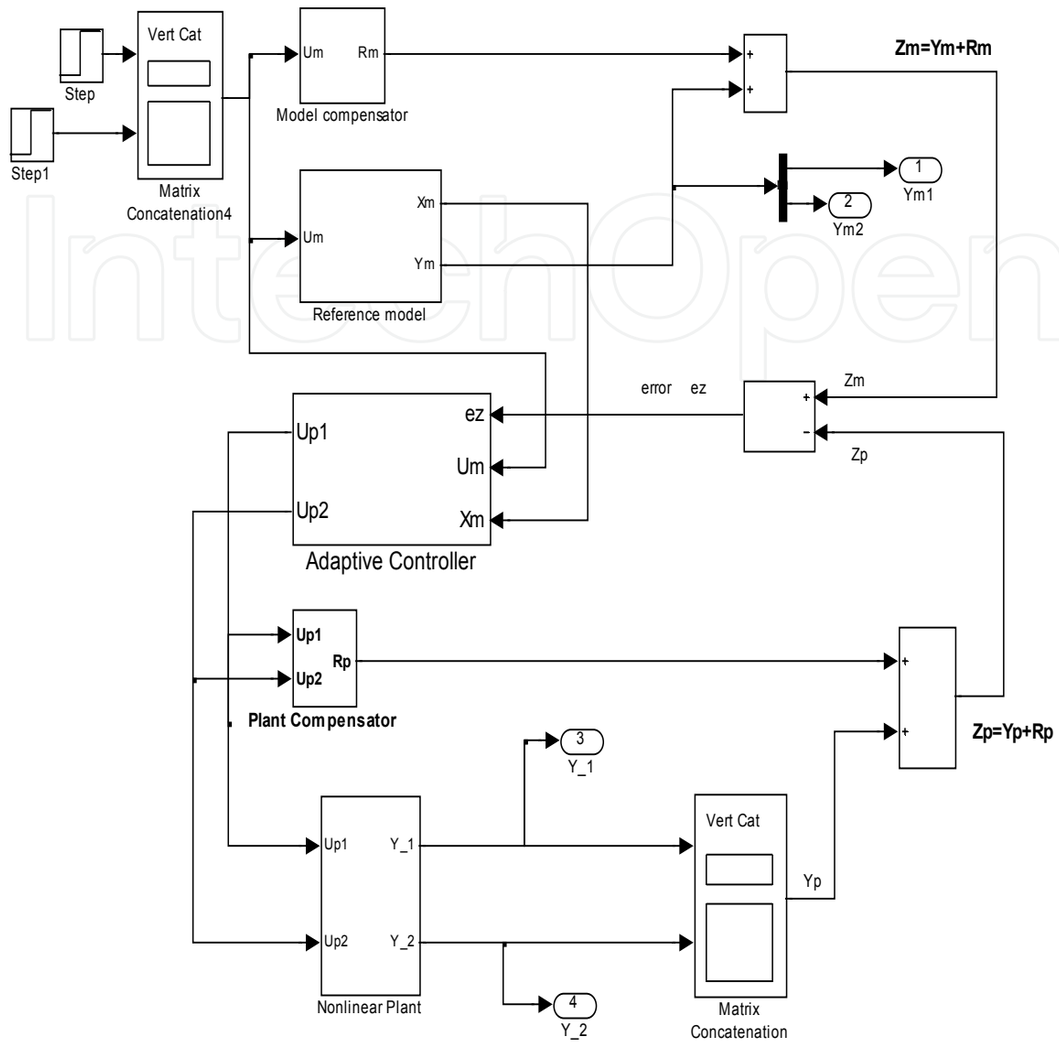

Fig. 8. Simulink Block Diagram of the overall control system with nonlinear plant.

4. Simulation Results

The nonlinear equations were used in building the plant in Simulink/MATLAB (Figure 8) and with the above described DMRAC algorithm, the following cases were simulated.

4.1 Case 1

- All initial conditions were set to zero.
- For both links the reference models were set to $G_{m1}(s) = G_{m2}(s) = 1/(30s+1)$
- For both links tip displacements were set to=0.05m
- Upper bound of plant parameters was used.

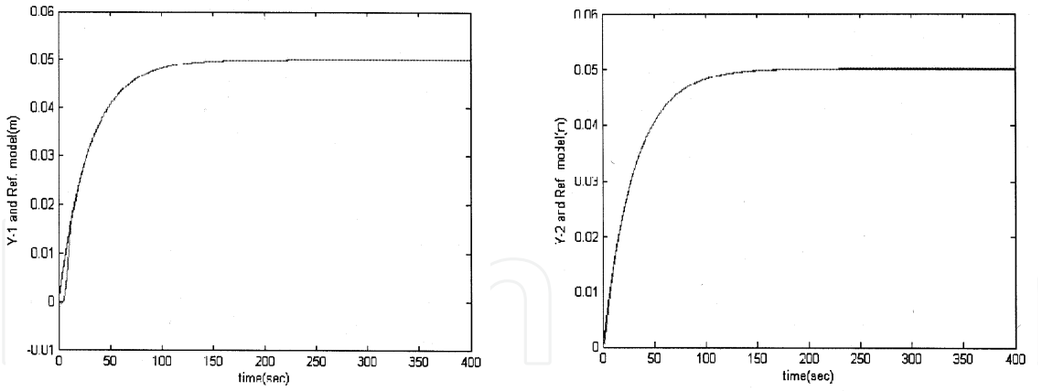

Fig. 9. Case 1: y_1 and reference model (left), y_2 and reference model (right)

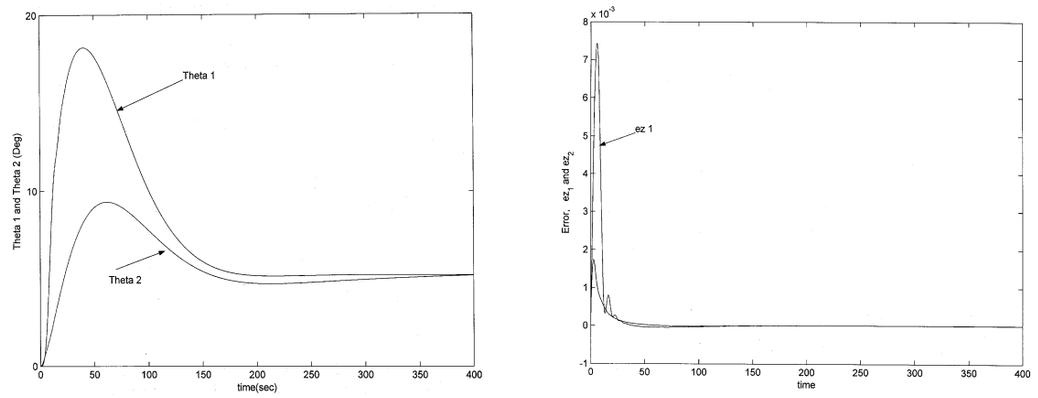

Fig. 10. Case 1: θ_1 and θ_2 (left), errors e_{z1} and e_{z2} (right)

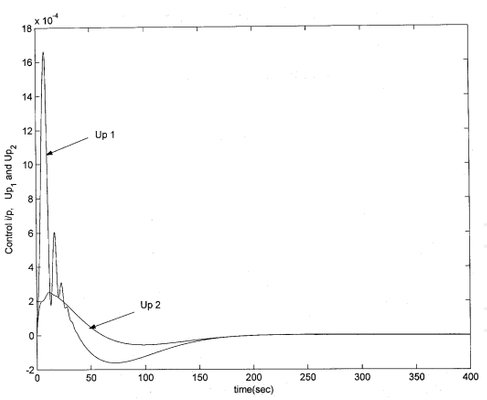

Fig. 11. Case 1: Control inputs, u_{p1} and u_{p2}

4.2. Case 2

- All initial conditions were set to zero.
- For both links the reference models were set to $G_{m1}(s) = G_{m2}(s) = 1/(15s+1)$
- For both links tip displacements were set to=0.05m
- Lower bound of plant parameters was used.

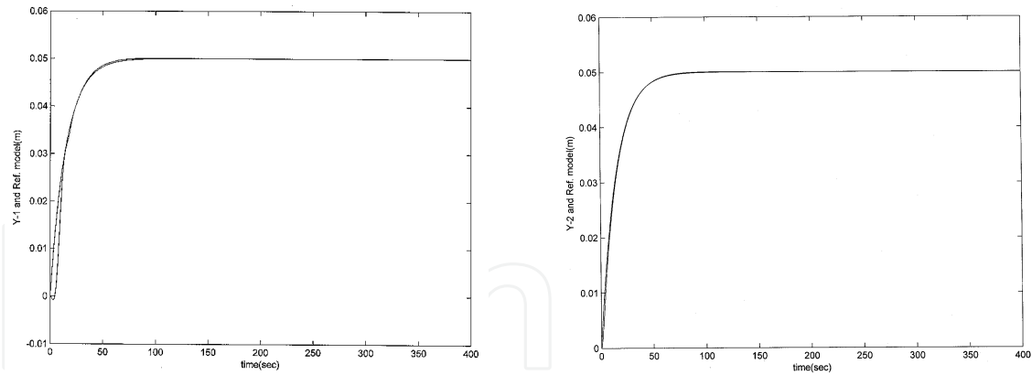

Fig. 12. Case 2: y_1 and reference model (left), y_2 and reference model (right)

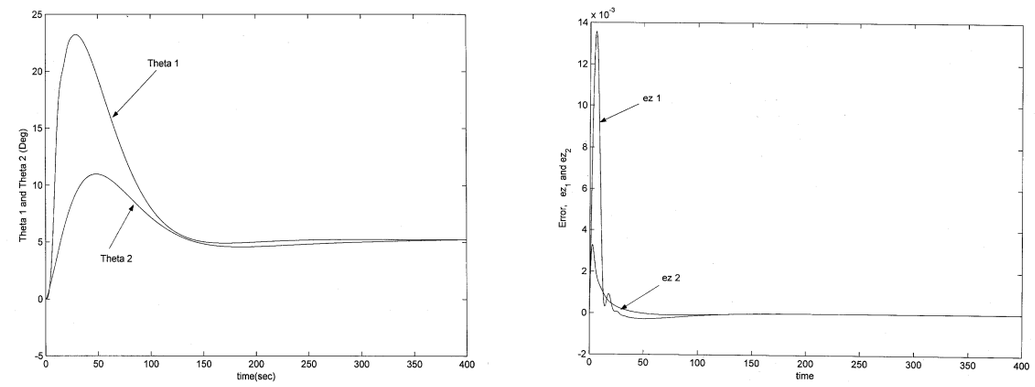

Fig. 13. Case 2: θ_1 and θ_2 (left), errors e_{z1} and e_{z2} (right)

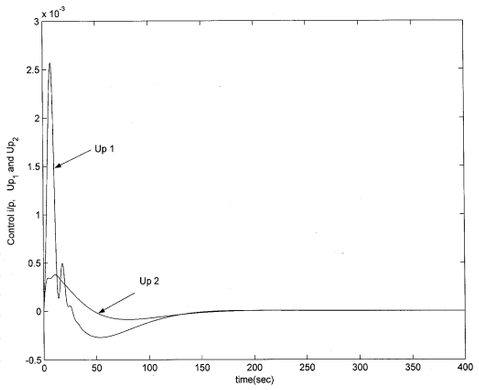

Fig. 14. Case 2: Control inputs, u_{p1} and u_{p2}

From the Figures 9-11 of Case 1 and the Figures 12-14 of Case 2, we can see that the tips of both links in each case follow the reference input. In Case 2 we have used a faster reference model to show the effectiveness of the DMRAC.

4.3. Case 3

- $\theta_1(0) = 5^\circ, \quad \theta_2(0) = 0^\circ$

- For both links the reference models were set to $G_{m1}(s) = G_{m2}(s) = 1/(30s+1)$
- For both links tip displacements were set to=0.01m
- Nominal set of plant parameters were used.

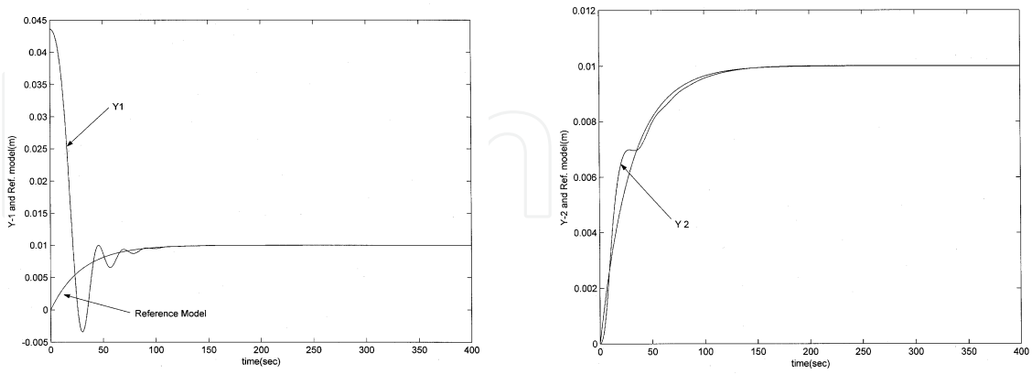

Fig. 15. Case 3: y_1 and reference model (left), y_2 and reference model (right)

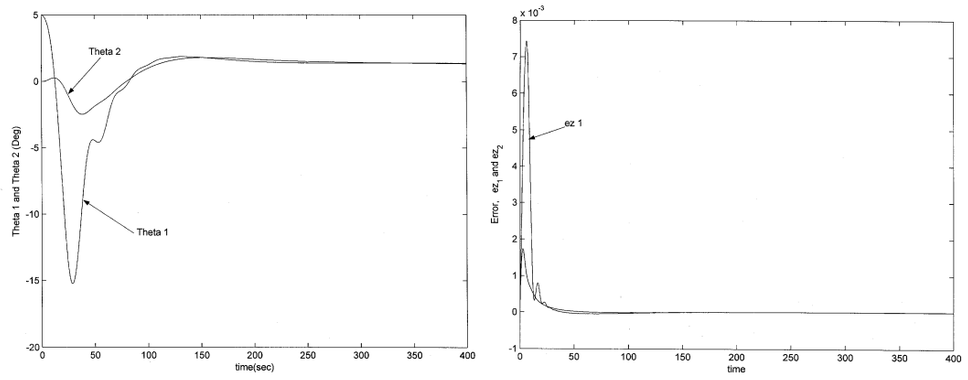

Fig. 16. Case 3: θ_1 and θ_2 (left), errors e_{z1} and e_{z2} (right)

From Figure 15 we see that at t=0, the tip position of link 2, y_2 begins at zero, however due to the initial condition for θ_1 tip position of first link, y_1 is displaced with respect to the desired reference model at t=0. From Figure 16 it is seen that θ_1 and θ_2 come to steady-state, while errors approach to zero.

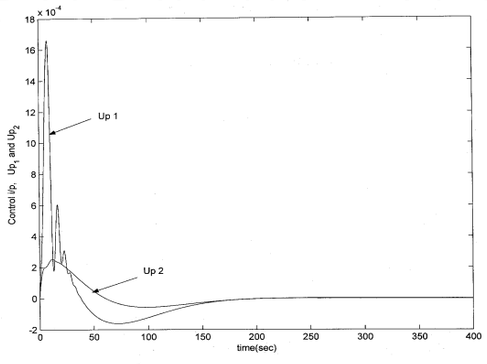

Fig. 17. Case 3: Control inputs, u_{p1} and u_{p2}

4.5. Case 4

- $\theta_1(0) = 0^\circ, \quad \theta_2(0) = 0^\circ$
- For both links the reference models were set to $G_{m1}(s) = G_{m2}(s) = 1/(50s+1)$
- For both links tip displacements were set to=± 0.01m
- Nominal plant parameters were used

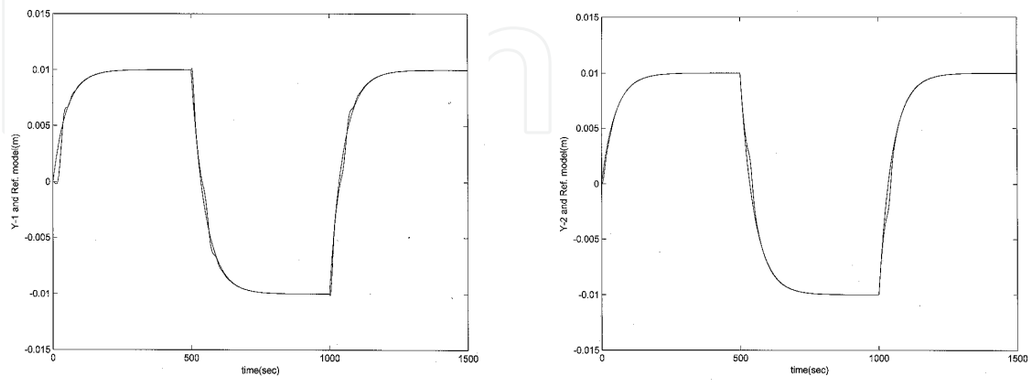

Fig. 18. Case 4: y_1 and reference model (left), y_2 and reference model (right)

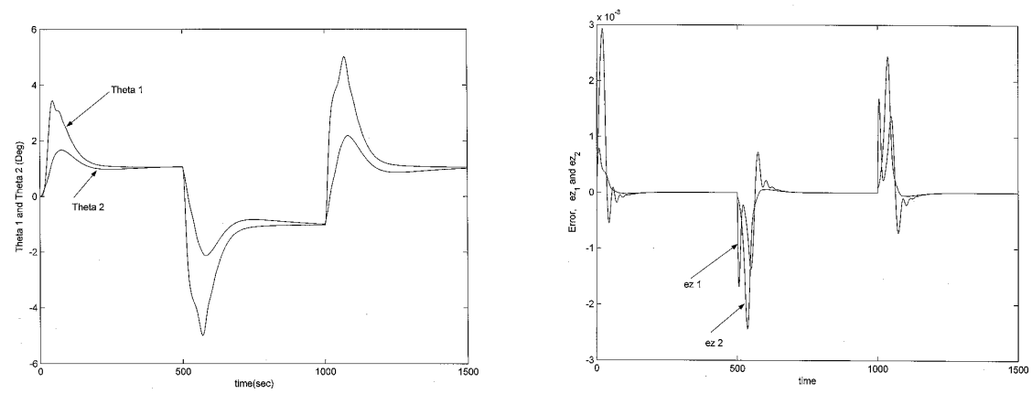

Fig. 19. Case 4: θ_1 and θ_2 (left), error e_z (right)

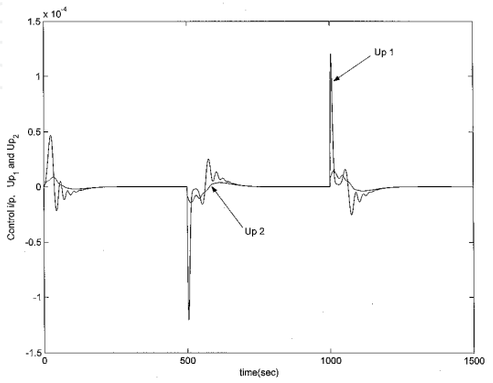

Fig. 20. Case 4: Control inputs, u_{p1} and u_{p2}.

5. Conclusions

Direct Model Reference Adaptive Control is utilized to control two-link flexible robot, whose parameters vary. The feedforward compensator was designed for the system and it was showed that the augmented plant satisfies the ASPR conditions over the range of parameter variations. As seen from the results of the tip position response, the system closely follows the reference model. During the simulations it was observed that DMRAC was capable of controlling the plant despite the changes in the plant parameters. The ease of its implementation and its robustness were demonstrated.

6. References

Cannon, R. H. & Schmitz, E. (1984). Initial Experiments on the End-Point Control of a Flexible One-Link Robot. *Int. J. Robotics Research*, Vol 3, No. 3, pages 325-338.

Geniele, H, Patel, R.V. & Khorasani, K. (1995). Control of a Flexible Link Manipulator. *IEEE Int. Conf. Robotics and Automation,* Vol. 1, pp 1217-1222, May 1995.

Ge, S. S., Lee, T.H. & Wang, Z. P. (2001). Adaptive Robust Controller Design for Multi-Link Flexible Robots. *Proceedings of the American Control Conference*, Vol. 2, pp 947-952, June, 2001.

Park, J. H. & Asada, H. (1992). Integrated Structure/Control Design of a Two-Link Nonrigid Robot Arm for High Speed Positioning, *IEEE Int. Conf. Robotics and Automation,* pp 735-741, Nice, France, May 1992.

Green, A. & Sasiadek, J. (2004). Dynamics and Trajectory Tracking Control of a Two-Link Robot Manipulator, *Journal of Vibration and Control*, Vol. 10, No. 10, 1415-1440.

Ider , K., S., Ozgoren, M., K. & Ay, O. (2002) Trajectory Tracking Control of Robots with Flexible Links, *Mechanism and Machine Theory,* Vol 37, pp 1377-1394.

Siciliano, B. & Villani, L. (2001). An Inverse Kinematics Algorithm for Interaction Control of a Flexible Arm with a Compliant Surface, *Control Engineering Practice,* Vol 9, pp 191-198.

De Luca, A. & Scicliano, B. (1989). Trajectory Control of a Nonlinear One-Link Flexible Arm *International Journal of Control,* Vol 50, pp 1699-1716.

Xu, B., Kenji, F. & Yoshikazun, H. (2005). An Energy-Based Nonlinear Control for a Two-Link Flexible Manipulator, *Trans Japan Soc Aeronautical Space Sc.*, Vol 48, No 160, pp. 92-101.

De Luca, A, Lucibello, P. & Nicolo, F. (1988). Automatic Symbolic Modeling and Non Linear Control of Robots with Flexible Links. *Proc. IEE Work On Robot Control,* pp. 62-70, Oxford, UK, April 1988.

Li, Y., Liu, G, Hong, T. & Liu, K. (2005). Robust Control of a Two-Link Flexible Manipulator with Quasi-Static Deflection Compensation Using Neural Networks, *Journal of Intelligent and Robotic Systems* Vol 44 , No 3 pp. 263-276. Kluwer Academic Publishers, MA, USA

Cetinkunt, S., Scicliano, B. & Book, J. W. (1984). Symbolic Modeling and Dynamic Analysis of Flexible Manipulators *Proc. IEEE Int. Conf. Syst., Man and Cyber.,*pp. 798-803, Georgia, USA.

Book, W., J. (1984). Recursive Lagrangian Dynamics of Flexible Manipulator Arms. *Int. Journal of Robotics Research,* Vol. 3, No. 3, pp. 87-101.

Miranda, E. (2004). Direct Adaptive Control of a Flexible Manipulator, *Thesis,* Texas A&M University, Kingsville, TX, USA.

Kaufman, H., Bar-Kana, I., & Sobel, K. (1998). *Direct Adaptive Control Algorithms: Theory and Applications,* Springer Communication and Control Eng., 2nd Edition, Springer-Verlag.

Ozcelik, S. & Kaufman, H. (1999). Design of robust direct adaptive controllers for SISO: time and frequency domain design conditions. *Intl. Journal of Control*, Vol.72, No. 6, pp. 517-530.

Ionnou, P. & Kokotovic, P. (1983). *Adaptive Systems with reduced models,* Springer-Verlag, New York, USA.

Bar-Kana, I. (1994). *Positive realness in multivariable stationary linear systems, Journal of Franklin Institute* ,No. 328, pp. 403-417.

Ozcelik, S. (2004). *Robust direct adaptive control for MIMO Systems Using Q-Parameterization*, *IFAC ALCOSP,* pp 93-98, Yokohama, Japan.

Adaptive Control

Edited by Kwanho You

ISBN 978-953-7619-47-3
Hard cover, 372 pages
Publisher InTech
Published online 01, January, 2009
Published in print edition January, 2009

Adaptive control has been a remarkable field for industrial and academic research since 1950s. Since more and more adaptive algorithms are applied in various control applications, it is becoming very important for practical implementation. As it can be confirmed from the increasing number of conferences and journals on adaptive control topics, it is certain that the adaptive control is a significant guidance for technology development.The authors the chapters in this book are professionals in their areas and their recent research results are presented in this book which will also provide new ideas for improved performance of various control application problems.

How to reference

In order to correctly reference this scholarly work, feel free to copy and paste the following:

Selahattin Ozcelik and Elroy Miranda (2009). Output Feedback Direct Adaptive Control for a Two-Link Flexible Robot Subject to Parameter Changes, Adaptive Control, Kwanho You (Ed.), ISBN: 978-953-7619-47-3, InTech, Available from: http://www.intechopen.com/books/adaptive_control/output_feedback_direct_adaptive_control__for_a_two-link_flexible_robot_subject_to__parameter_changes

INTECH
open science | open minds

InTech Europe
University Campus STeP Ri
Slavka Krautzeka 83/A
51000 Rijeka, Croatia
Phone: +385 (51) 770 447
Fax: +385 (51) 686 166
www.intechopen.com

InTech China
Unit 405, Office Block, Hotel Equatorial Shanghai
No.65, Yan An Road (West), Shanghai, 200040, China
中国上海市延安西路65号上海国际贵都大饭店办公楼405单元
Phone: +86-21-62489820
Fax: +86-21-62489821

IntechOpen